EOS/AMSR RAINFALL

Algorithm Theoretical Basis Document

Version 2 GPROF2010 L2A
November, 2014

Christian Kummerow, Ralph Ferraro and David Randel

TABLE OF CONTENTS

1.0 INTRODUCTION

1.1 Objectives

The AMSR-E instrument is a multichannel passive microwave radiometer flying on the EOS Aqua spacecraft. As a science mission with integrated applications goals, Aqua will advance understanding of the Earth's water and energy cycle and extend current capabilities in using accurate and timely information of precipitation to directly benefit the society. The current Algorithm Theoretical Basis Document (ATBD) deals with the precipitation product from the AMSR-E sensor. The passive microwave algorithm is designed to take advantage of a previously constructed *a-priori* database of TRMM observed precipitation profiles and their associated brightness temperature signals. These databases are then used in conjunction with Bayesian inversion techniques. The specific implementation is described below.

1.2 Purpose

This ATBD describes the AMSR-E passive microwave rainfall algorithm. It represents GPROF 2010 V2 of the algorithm. The output parameters of the algorithm are enumerated in Table 1. This document identifies the physical theory upon which the algorithm is based and the specific sources of input data and output from the retrieval algorithm. The document includes implementation details, as well as the assumptions and limitations of the adopted approach.

Table 1. Key output parameters from the Level 2A Rainfall Product.

Pixel Information		
Parameter	**Units**	**Comments**
Latitude, longitude	Deg.	Pixel earth coordinate position
Pixel Status	None	Identifies pixels eliminated by QC procedures
Surface Type	None	land surface emissivity class/ocean/coast/sea ice
Quality Flag	None	Pixels w/o good T_b matches in database
Precipitation Probability	0-1 Fraction	Fraction of pixels in Bayesian average that have precipitation
Surface Precipitation	mm/hr	Total Precipitation
Convective Precipitation	mm/hr	Surface Precip that is convective
Surface Rain	mm/hr	Liquid portion of the Total Precipitation
Cloud Water Path, Rain Water Path, Ice Water Path	Kg/m^2	Integrated from retrieved profile

1.3 Scope

This document covers the theoretical basis for the retrieval of liquid and solid precipitation from the AMSR-E radiometers. The algorithm is a Bayesian type algorithm. The algorithm searches an *a-priori* database of potential rain profiles and retrieve a weighted average of these entries based upon an uncertainty weighted proximity of the observed T_b to the simulated T_b corresponding to each rain profile. The *a-priori* information is supplied by the TRMM radar/radiometer algorithm as detailed in Kummerow et al., (2010). The mathematics of Bayesian inversions are well understood. The solution provides a mean rain rate as well as its uncertainty. The major sources of systematic errors in these algorithms are the quality of the *a-priori* database; the estimate of the forward model uncertainty; and the ancillary information used to subset the *a-priori* database.

Section 1 describes the objectives, purpose and scope of the document. Section 2 provides AMSR-E satellite instrumentation background. The process concepts and algorithm descriptions for the geophysical parameters of the rainfall product are presented in Section 3. Section 4 describes the algorithm infrastructure, while Section 5 summarizes the assumptions and limitations.

2.0 INSTRUMENT CHARACTERISTICS

The AMSR-E instrument is a twelve channel, six frequency total power passive microwave radiometer system. It measures brightness temperatures at 6.925, 10.65, 18.7, 23.8, 36.5, and 89.0 GHz. Vertically and horizontally polarized measurements are taken at all channels.

The instrument, modified from the design used for the ADEOS-II AMSR, consists of an offset parabolic reflector 1.6 meters in diameter fed by an array of six feedhorns. The reflector and feedhorn arrays are mounted on a drum, which contains the radiometers, digital data subsystem, mechanical scanning subsystem, and power subsystem. The reflector/feed/drum assembly is rotated about the axis of the drum by a coaxially mounted bearing and power transfer assembly. All data, commands, timing and telemetry signals, and power pass through the assembly on slip ring connectors to the rotating assembly.

A cold load reflector and a warm load are mounted on the transfer assembly shaft and do not rotate with the drum assembly. They are positioned off axis such that they pass between the feedhorn array and the parabolic reflector, occulting it once each scan. The cold load reflector reflects cold sky radiation into the feedhorn array thus serving, along with the warm load, as calibration references for the AMSR-E. Calibration of the radiometers is essential for collection of useful data. Corrections for spillover and other antenna pattern effects are incorporated in the data processing algorithms.

The AMSR-E rotates continuously about an axis parallel to the local spacecraft vertical at 40 rpm. At an altitude of 705 km, it measures the upwelling scene brightness temperatures over an azimuthal range of +/- 70 degrees about the sub-satellite track, resulting in a swath width of 1500 km.

During a period of 1.5 seconds the spacecraft sub-satellite point travels 10 km. Even though the instantaneous field-of-view for each channel is different, active scene measurements are recorded at equal intervals of 10 km (5 km for the 89 GHz channels) along the scan. The half cone angle at which the reflector is fixed is 46.6 degrees which results in an Earth incidence angle of 53.8 degrees. Table 2 lists the pertinent performance characteristics.

Table 2. AMSR-E PERFORMANCE CHARACTERISTICS

Center Frequency (GHz)	6.925	10.65	18.7	23.8	36.5	89.0
Bandwidth (MHz)	350	100	200	400	1000	4000
Sensitivity (K)	0.3	0.6	0.6	0.6	0.6	1.1
IFOV(km x km)	76 x 44	49 x 28	28 x 16	31 x 18	14 x 8	6 x 4
Sampling rate (km x km)	10 x 10	10 x 10	10 x 10	10 x 10	10 x 10	5 x 5
Integration Time (msec)	2.6	2.6	2.6	2.6	2.6	1.3
Main Beam Efficiency (%)	95.3	95.0	96.3	96.4	95.3	96.0
Beamwidth (degrees)	2.2	1.4	0.8	0.9	0.40	0.18

3.0 ALGORITHM DESCRIPTION

3.1 Ocean Algorithm

The AMSR-E radiometer ocean algorithm is based upon a Bayesian approach in which the TRMM satellite is used to create an *a-priori* database of observed cloud and precipitation profiles as described in Kummerow et al., (2010). Once a database of profiles and associated brightness temperatures is established, the retrieval employs a straightforward Bayesian inversion methodology. In this approach, the probability of a particular profile **R**, given $\mathbf{T_b}$ can be written as:

$$\Pr(\mathbf{R} \mid \mathbf{T_b}) = \Pr(\mathbf{R}) \times \Pr(\mathbf{T_b} \mid \mathbf{R}) \qquad (1)$$

where Pr(**R**) is the probability that a certain profile **R** will be observed and Pr($\mathbf{T_b}$ | **R**) is the probability of observing the brightness temperature vector, $\mathbf{T_b}$, given a particular rain profile **R**. The first term on the right hand side of Eqn. (1) is derived from the *a-priori* database of rain profiles established by the radar/radiometer observing systems discussed in section 3.1. The second term on the right hand side of Eqn. (1), is obtained from radiative transfer computations through the cloud model profiles. The formal solution to the above problem is presented in detail in Kummerow *et al*., (1996). In summary, the retrieval procedure can be said to compose a new hydrometeor profile by taking the weighted sum of structures in the cloud structure database that are radiometrically consistent with the observations. The weighting of each model profile in the compositing procedure is an exponential factor containing the mean square difference of the sensor observed brightness temperatures and a corresponding set of brightness temperatures obtained from radiative transfer calculations through the cloudy atmosphere represented by the model profile. In the Bayesian formulation, the retrieval solution is given by:

$$\hat{E}(R) = \sum_j R_j \frac{\exp\left\{-0.5\left(Tb_o - Tb_s\left(R_j\right)\right)^T (O+S)^{-1}\left(Tb_o - Tb_{s(R_j)}\right)\right\}}{\hat{A}} \qquad (2)$$

Here, R_j is once again the vector of model profile values from the *a-priori* database model, Tb_o is the set of observed brightness temperatures, $Tb_s\left(x_j\right)$ is the corresponding set of brightness temperatures computed from the model profile R_j. The variables *O* and *S* are the observational and model error covariance matrices, respectively, and $\hat{A}$ is a normalization factor. The profile retrieval method is an integral version of the well-

known minimum variance solution for obtaining an optimal estimate of geophysical parameters from available information (Lorenc, 1986, for a general discussion).

While the mechanics of Bayesian inversions are fairly well understood, the AMRE-E code does not search the entire a-priori database but instead searches only a subset of profiles with coincident Sea Surface Temperature (Tskin) and Total Column Water Vapor (TCWV). Previous studies such as Berg et al. (2006) have shown that searching only over the appropriate SST and TCWV over oceans constrains the solution in a significant and positive manner. An important step is, therefore, to select the appropriate *a-priori* databases in the Bayesian inversion. TCWV is internally within the AMSR-E precipitation algorithm using an Optimal Estimation (OE) framework developed by Elsaesser and Kummerow (2008), while SST is obtained from (Reynolds *et al.* 2006) daily climatology. The same OE-based TCWV and SST climatology is also attached to the a-priori database to ensure consistency between the brightness temperatures.

The coverage of TRMM is limited to the tropics : 36^{o}N – 36^{o}S. This limits the number of cold surface temperatures and associated TCWV amounts that TRMM sees. It does however, cover the tropical ocean masses exceedingly well. Additional colder synthetic profiles are created using the original PR profiles. Here, lower layers of the profiles are removed in order to simulate sea surface temperatures at 281, 278, and 275 degrees ^{o}K.

3.2 Land Algorithm

Rainfall retrievals over land, as discussed in the following sections, are far more difficult than oceanic retrievals due to the large and variable emissivity of the land surface. Specifically, the high emissivity masks the emission signature that is related directly to the water content in the atmosphere. Instead, only the brightness temperature depression due to scattering in the upper portion of clouds is observed. The scattering increases with increasing frequencies. Consequently, brightness temperature depressions at the 89 GHz channel of AMSR-E will contain the least ambiguous signal of scattering by ice and/or large raindrops. The brightness temperature depression will be converted to an expected rainfall rate through the GPROF retrieval scheme where databases of hydrometeor profiles (associated with a variety of rain systems) will be developed for different climatological zones. Recent results from TRMM indicate that the relationship of lightning flashes (which is highly correlated with the 85 GHz scattering signature) and rainfall varies over the global land regions

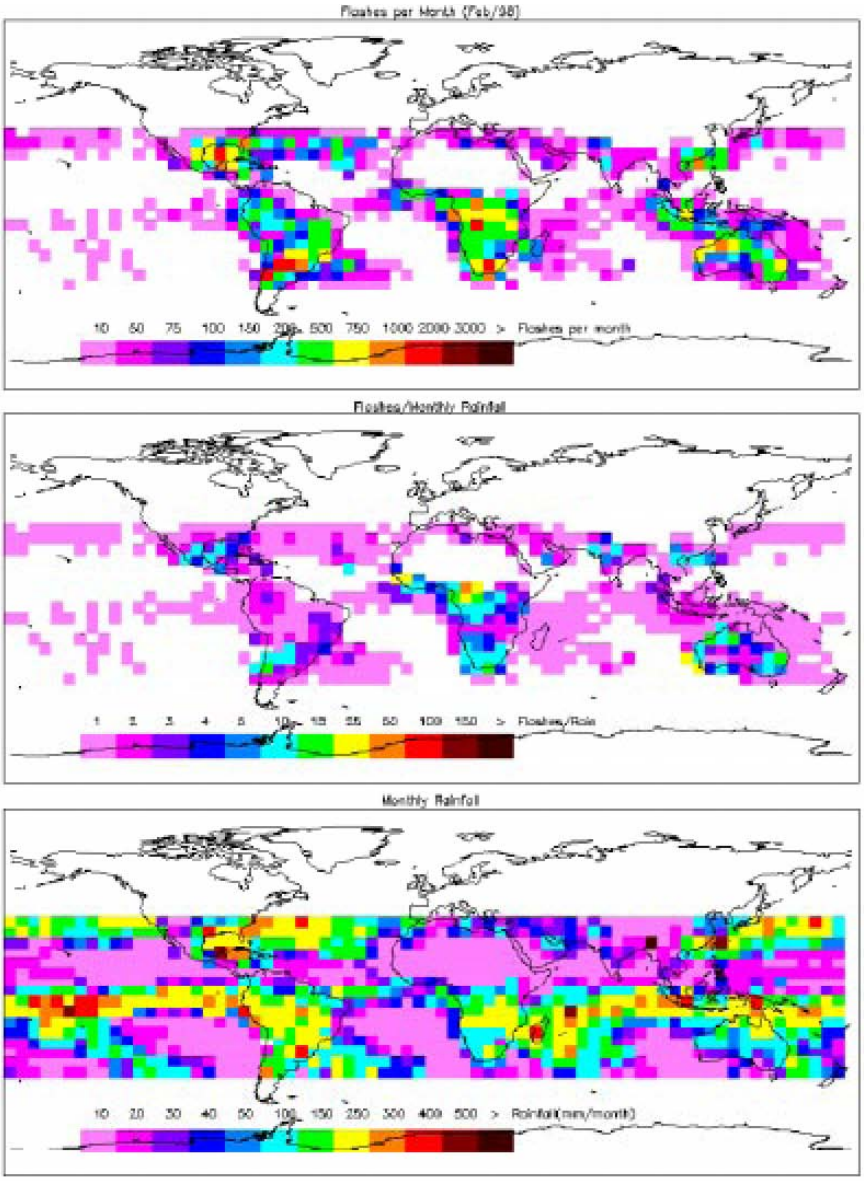

Figure 1: Relationships between lightning and rainfall derived by TRMM. Top panel: number of lightning strikes per 5^{o} x 5^{o} grid box for February 1998. Middle panel: ratio of lightning to rainfall. Bottom panel: Total rainfall derived for the TRMM radar for February 1998.

For example, note how the monthly rainfall in tropical South America and Africa are fairly similar, yet, the amount of lightning in Africa is much larger. In this instance, the globally applied relationship between scattering and rainfall is likely erroneous in Africa. Development of profile databases for different climatological zones can account for these differences. However, as a starting point, we will insure that these retrievals match

closely with established algorithms developed for the SSM/I and TMI sensors at the time of EOS-PM launch. Details on this procedure follow.

A further complication that arises over land is the lack of consistent backgrounds against which to compare the *Tb* depression. To alleviate this problem caused by the varying emissivity associated with changes in surface characteristics (e.g., surface wetness, snow cover, vegetation, etc.), a rain/no-rain temperature depression threshold is required. Additionally, snow and desert surfaces cause depressed *Tb's* at high frequencies (due to surface volume scattering) and can be confused with the rain signature. If these surface types are not properly screened, they can be misinterpreted as ice scattering in clouds.

3.2.1 Land Rainfall – Rain/No Rain determination

The "screening" issue has always been one of modest controversy in the land-based retrievals because of the empirical nature of their form. Intuitively, one immediately thinks that such screens will vary greatly with sensor. However, as is described later, these screens (i.e., *Tb* relationships separating rainfall from other surfaces) seem to hold valid for other sensors, with only minor modifications needed. Additionally, one school of thought in physical retrievals is that the rain rate retrieval becomes a two-step process: rain identification and rain rate determination. This philosophy has been adopted by GPROF and is being utilized for the AMSR-E retrieval algorithm.

The basis for the retrieval over land comes from the work of Grody (1991), who developed a global scattering index (*SI*) at 85 GHz for use with the SSM/I sensor. Further refinement of the technique is described in Ferraro *et al*. (1994) and Ferraro *et al*. (1998). The rationale was to first develop a relationship which could best predict the 85 GHz *Tb* under "non-scattering" conditions for the land surface in question. Then, by estimating this value and subtracting the actual 85 GHz *Tb*, a measure of the depression due to scattering by precipitation ice/rain drops could be determined. The form of the *SI* is as follows:

$$SI_{85V} = a + b \cdot Tb_{19V} + c \cdot Tb_{22V} + d \cdot Tb_{22V}^2 - Tb_{85V} \qquad (3)$$

where the coefficients *a*,*b*,*c*, and *d* were derived by assembling a global data set of SSM/I

observations under scatter-free conditions. Through an exhaustive evaluation, Grody (1991) found that an *SI* value of 10 K or greater was a good, global indicator of rain. A lower threshold does detect more rain; however, it also causes the detection of false alarms to increase. Because snow and deserts can cause a similar scattering signature, a set of "screens" were developed to remove such features. The desert check involves the use of polarization information at 19 GHz, while the separation of rain from snow utilizes two relationships involving the *Tb* at 22 and 85 GHz.

Ferraro *et al*., (1994), built upon the Grody (1991) study, and developed a more robust set of relationships to be used for the detection of rain over land from the SSM/I. In addition, the original relationships derived by Grody (1991) used antenna temperatures which were convolved to the 19 GHz *FOV*; the updated study used the more conventional *Tb* values and preserved the original SSM/I footprint sizes, allowing for easy implementation by the scientific community. The new land relationship is given by:

$$SIL = 451.9 - 0.44 \cdot Tb_{19V} - 1.775 \cdot Tb_{22V} + 0.00575 \cdot Tb_{22V}^2 - Tb_{85V} \qquad (4)$$

This study also re-derived the relationships to separate rain from snow and deserts and introduced a new screen for semi-arid regions (i.e., the Sahel region of Africa). In summary, the *SI* values greater than 10K identify rain areas, and subsequent screens remove snow covered, desert, and semi-arid land regions.

McCollum *et al*. (1999) used SSM/I data to optimize two screening methodologies described in Ferraro *et al*. (1998) and to evaluate both methods to document and improve their deficiencies. The two methodologies are the NESDIS screening of Ferraro (1997) and the GSCAT2 screening used in GPROF 4.0 algorithm, and at this writing, in TRMM TMI production algorithm. In general, the NESDIS based screening tends to be more liberal in nature and allows for rain identification in colder environments (at the expense of misclassification due to melting snow) while GPROF is more conservative, and flags these areas as indeterminate (at the expense of eliminating moderate to heavy rainfall in winter seasons). GPROF also appears to suffer from some inadequate screening in semi-arid areas. McCollum *et al*. (1999) developed a methodology that adopts the more conservative GPROF approach but uses spatial information from neighboring pixels to "fill-in" indeterminate areas. An additional modification to previous rain/no-rain temperature depression thresholds was made. In a departure from the scattering index

(Eq. 3) threshold, which was determined specifically for SSM/I data, a more generic difference between low and high frequency SSM/I channels is used. A 22V - 85V threshold of 8K was found to be appropriate for identification of pixels with rain.

Shown in Figure 2 is an example of rainfall rates from the NESDIS, GPROF, and screens for an SSM/I overpass January 2, 1999. This figure illustrates the benefit of the new screen. The snow line was near the Indiana/Kentucky border that day, so ideally there would be estimates south of the snow line and no estimates (indeterminate) north of this line. The original screens classify all but the southernmost areas of the rainfall as indeterminate, while the new screen captures the true rainfall up until just south of the true snow line.

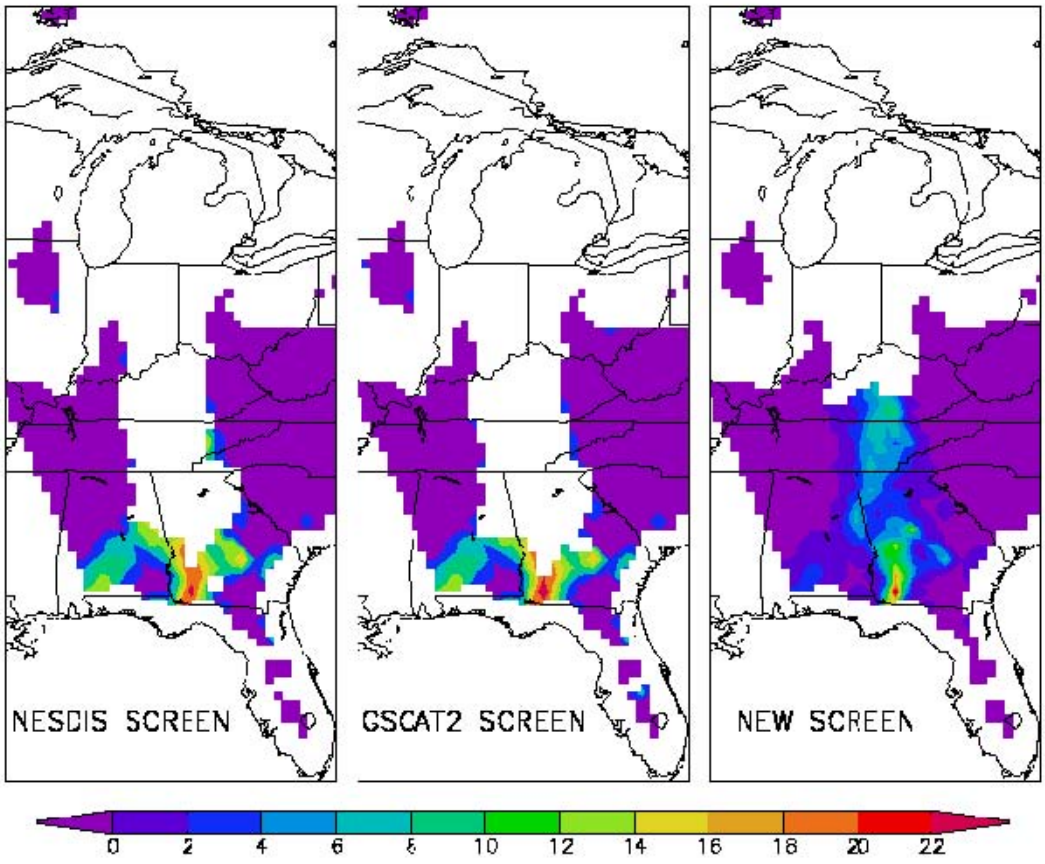

Figure 2. Comparison of rainfall rates (mm/h) from GPROF with different screens for an SSM/I overpass on January 2, 1999. Rainfall rates are in mm/h.

3.2.2 Land Algorithm – Rain Rate Determination

Because of the non-uniqueness in resolving proper hydrometeor profiles, based on SSM/I measurements, the use of physical retrieval algorithms over land has been limited. Although the proper surface rain rates may be retrieved by matching the observed *Tb's* to model simulations, the intervening atmospheric cloud constituents are typically incorrect due to the lack of information available from the SSM/I. An alternative method to retrieve rain rate has been to calibrate the *SI* with ground-based radar measurements from the United States, Japan, and the United Kingdom (Ferraro and Marks, 1995). Specifically, the following relationship was found to work best for global applications:

$$RR(mm/hr) = 0.00513 \cdot SIL^{1.9468} \qquad (5)$$

where *RR* is in mm/hr. Since these relationships increase rapidly for higher values of *SIL*, any retrieval above 35 mm/hr is set to 35 mm/hr. Although somewhat arbitrary, practice shows that this is the upward limit of rain rates retrievable from the 85 GHz measurements (e.g., the maximum mean rain rate that could exist in a 13 by 15 km *FOV*). Using the 10K minimum threshold for the *SIL* values, the minimum retrievable rain rate is approximately
0.5 mm/hr. This algorithm was implemented by FNMOC in 1995 as the operational SSM/I rain rate algorithm, and continues to operate in that capacity. In addition, the monthly derived rainfall from this algorithm (Ferraro, 1997) is used as a component of the GPCP blended analysis (Huffman *et al*., 1996), is continually updated, is archived at the National Climatic Data Center
(http://www.ncdc.noaa.gov/ol/satellite/ssmi/ssmiproducts.html), and can be examined interactively on the world wide web at http://orbit35i.nesdis.noaa.gov/arad2/index.html. The AMSR-E instrument will contain slightly different frequencies than the SSM/I (e.g., 89.0 instead of 85.5 GHz), contain more information (e.g., 10 channels vs. 7), and will also have significantly higher spatial resolution. Because of these attributes, we feel that there will be an improved ability to retrieve hydrometeor profiles from the AMSR-E, although the ocean retrievals will still be more accurate. It is therefore convenient to have a physical basis for modifying SSM/I algorithms to suit the AMSR-E observations. To accomplish this, as well as to simplify the retrieval process, the AMSR-E precipitation team decided to use the same GPROF retrieval methodology as used for the ocean retrieval. Unlike the ocean component, however, the initial database of possible profiles

was carefully selected to include only those profiles that fit the empirical relation given in Eq'n (5). The relationship of (eq'n 5) was reproduced by selecting 36 profiles fitting (eq'n 5) from the several thousand profiles in the GPROF database (McCollum *et al*. 1999).

A sample comparison of daily, 0.25° rainfall estimates from global SSM/I data from March 8-10, 1999, is shown in Figure 3. As with all other days tested, there is very close correspondence between the GPROF rainfall estimates using the new profile database and the Ferraro (1997) algorithm estimates produced from (4), so it appears the GPROF algorithm using the new database is successful in producing similar rainfall estimates as the NESDIS algorithm for SSM/I data. The profiles selected for the SSM/I retrievals can then be used in a straightforward manner to compute the relations needed for the slightly different frequencies of AMSR-E. Resolution and additional channel measurement advantages can likewise be addressed through the cloud models and TRMM TMI and profiling radar measurements.

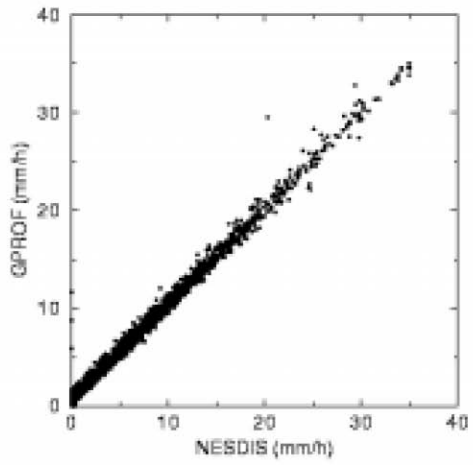

Figure 11: Comparison of 0.25° daily rainfall rates March 8-10, 1999) from the NESDIS empirical algorithm and from the GPROF algorithm with the new profile database.

3.2.3 Land Algorithm - Summary

For several years (1987 – 96), the SSM/I was the only passive microwave sensor that was operating. Beginning with TRMM (1997) and AMSU (1998), we are now in an era with

multiple sensors in operation. Hence, the need for a "unified" retrieval algorithm that incorporates the best features of several existing algorithms, as well as one that is built in a framework that allows for continual enhancements is highly desirable. The AMSR-E rainfall team has adopted this philosophy and believes that the development of a unified land based retrieval algorithm for use with a variety of passive microwave sensors has several advantages. First, the same underlying physical assumptions (i.e., hydrometeor profiles, radiative transfer, etc.) are consistent. This allows for a more direct approach for evaluating and ultimately improving the retrieval process. These improvements can all be incorporated via the cloud model database and surface type/climate zone classification in the land retrieval module. The second advantage is that the module will be fully portable to other sensors, and will be suitable for operational/production use. This point cannot be stressed enough, as user friendly code is critical for a 24-hour a day, 7 day a week operation. Experience with SSM/I, TMI, and AMSU shows that even the smallest change to a software module can cause havoc in an operational environment! Finally, the implemented code will be the same for both land and water. This will greatly simplify the algorithm flow, thus enhancing our confidence that the code will work as intended.

4.0 Output Variables and Flags

4.1 Orbit Header Record Variable Specifications

Satellite
3 letter code for the satellite which produced the data. Valid strings: AME

Sensor
Satellite Sensor, valid strings: AMSR-E

Algorithm Version
GPROF 2010 Version which produced the output file.

Pre Processor Version
GPROF 2010 Pre-Processor version number

Ocean Data base
File name of the ocean profile database

Original Radiometer Input Filename
File Name of the original; input data file.

Start Date/Time
Start date and time of first scan in file. Defined as the date/time structure which holds six integer*2 values - year, month, day, hour, minute, second.

Creation Date/Time
Start date and time of file creation. Defined as the date/time structure which holds six integer*2 values - year,month,day,hour,minute,second.

Granule
Generally this is defined as the satellite orbit number since launch.

Missing Data Value
Value of the floating point missing data .

Num Scans, Num Pixels
Number of Scans, Pixels in each scan

Error Comment1
Available open space for various comments and spare bytes.

4.2 Scan Data Record Variable Specifications

Time
year, month, day, hr, min, sec - Int*2(6)
TAI93
time in seconds since 1/1/93 - real*8

4.3 Pixel Data Record Variable Specifications

Latitude, Longitude
Pixel latitude and longitude.

pixel Status
If there is no retrieval at a given pixel, pixelStatus explains the reason.

0 : Valid pixel
1 : Boundary error in landmask
2 : Boundary error in sea-ice check
3 : Boundary error in sea surface temperature
4 : Invalid time
5 : Invalid latitude/longitude
6 : Invalid brightness temperature
7 : Invalid sea surface temperature
8 : No retrieval due to sea-ice over water
9 : No retrieval due to sea-ice over coast
10 : Land/coast screens not able to be applied
11 : Failure in ocean rain - no match with database profile Tbs

surface Type
Surface type codes are as follows:

10 : Ocean
11 : Sea ice
12 : Partial sea ice
20 : Land
30 : Coast
31 : Inland water

quality Flag

qualityFlag indicates a generalized quality of the retrieved pixel. Values follow:

Ocean Algorithm:

High: Good retrieval (uses entries from TRMM apriori database)

Medium: Retrieval used extended database and/or expanded search radius for apriori database (see oceanExtendedDbase and/or oceanSearchRadius)

Low: Retrieval used search radius to find matches in apriori database (see oceansearchRadius)

Land/Coast Algorithm:

High: Good retrieval

Medium: Ambiguous pixel (see landScreenFlag)

Low: Missing or unable to retrieve pixels (see pixelStatus)

Valid values include:

0 : High quality (retrieval is good)

1 : Medium quality (use with caution)

2 : Low quality (recommended qualitative use only)

land Ambiguous Flag

Defines codes for uncertain/ambiguous retrievals over land. Valid values are:

0 : No information

13 : Ambiguous T22V / 2 different scattering screens

14 : Cannot discriminate precip from cold surface

63 : Light precipitation

64 : Cold surface

65 : Grody light precipitation

66 : Huffman ambiguous

land Screen flag

0 : No information

-31 : Land retrieval found ice likely

-41 : Land retrieval found large polarization difference due to ice or sand

-51 : Warm 85H and Low 22V, or clear ocean likely in coast retrieval

-61 : probable coastline in coast retrieval

ocean Extended Dbase

Percent of the extended database entries (i.e., beyond the TRMM database) used in the retrieval (Range 0 - 100).

0 : Only the TRMM database entries are used

1-99 : % of the entries from the extended database are used

100 : Only the extended database entries are used

ocean Search Radius
Expansion of the search radius of the apriori database beyond the initial SST and TPW search range. The profiles for the rain ocean procedure are grouped by SST and TPW. The individual pixels TPW and SST are used to retrieve a group of pixels from the database. If there are fewer than 1000 profile clusters found, the search radius is expanded. Valid values are:

0 : Default search radius used
1 : Search radius expanded by +/- 1 mm in TPW and +/- 1 degree in SST
N : Search radius expanded by +/- N mm in TPW and +/- N degrees in SST

chi Squared
Error diagnostic for Optimal Estimation calculation of TPW and wind speed. Values greater than the number of channels (9 for TMI) should be considered suspect, with values greater than 18 of limited use. Rainfall is possible above these values. Values could range from 0 to 10000, but should be less than 100.

probability Of Precip
A diagnostic variable, in percent, defining the fraction of raining vs. non-raining Dbase profiles that make up the final solution. Values range from 0 to 100 percent.

sun Glint Angle
Conceptually, the angle between the sun and the instrument view direction as reflected off the Earth's surface. More specifically, define a Sun Vector from the viewed pixel location on the earth ellipsoid-model surface to the sun. Also define an Inverse Satellite Vector from the pixel to the satellite. Then reflect the Inverse Satellite Vector off theearth's surface at the pixel location to form the Reflected Satellite View Vector. sunGlintAngle is the angular separation between the Reflected Satellite View Vector and the Sun Vector. When sunGlintAngle is zero, the instrument views the center of the specular (mirror-like) sun reflection. Values range from 0 to 180 degrees.

freezing Height
The height, in meters, of the 0oC isotherm above the earth ellipsoid.

surface Precipitation, convective Precipitation
The instantaneous total precipitation and convective precipitation at the surface for each pixel. Check pixelStatus for a valid retrieval. Values are in mm/hr.

surface Rain
The instantaneous rain rate (liquid portion of precipitation) at the surface for each pixel. Check pixelStatus for a valid retrieval. Values are in mm/hr.

cloud Water Path, rain Water Path, Ice Water Path
Total cloud liquid water, total rain water and total cloud ice in the column. Values range from 0 to 3.0 kg/m2.

5. 0 REFERENCES

Berg, W., T. L'Ecuyer, and C. Kummerow, 2006. Rainfall climate regimes: The relationship of regional TRMM rainfall biases to the environment, *J. Appl. Meteor. Climatol.*, **45**, 434–454.

Elsaesser, G.S. and C.D. Kummerow, 2008. Toward a fully parametric retrieval of the nonraining parameters over the global oceans, *J. Appl. Meteor. Climatol.*, **47**, 1599–1618.

Ferraro, R.R., N.C. Grody, and G.F. Marks, 1994: Effects of surface conditions on rain identification using the SSM/I, *Rem. Sens. Rev.*, **11**, 195-209.

Ferraro, R.R. and G.F. Marks, 1995: The development of SSM/I rain rate retrieval algorithms using ground based radar measurements. *J. Atmos. Oceanic Technol.*, **12**, 755-770.

Ferraro, R.R., 1997: SSM/I derived global rainfall estimates for climatological applications. *J. of Geophys. Res,* **102**, 16,715-16,735.

Ferraro, R.R., E.A. Smith, W. Berg, and G. Huffman, 1998: A Screening Methodology for Passive Microwave Precipitation Retrieval Algorithms. *J. Atmos. Sci.*, 55, 1583-1660.

Goody, R. M., and Y. L. Yung, 1989: Atmospheric Radiation. Oxford University Press, pp. 330-337. Grody, N.C., 1991: Classification of snow cover and precipitation using the Special Sensor Microwave/Imager (SSM/I). *J. of Geophys. Res.*, **96**, 7423-7435.

Huffman, G.J., R.F. Adler, P. Arkin, A. Chang, R. Ferraro, A. Gruber, J. Janowiak, A. McNab, B. Rudolf, and U. Schneider, 1996: The global precipitation climatology project (GPCP) combined precipitation data set. *Bull. Amer. Meteor. Soc.*, *78*, 5-20.

Kummerow, C., W. S. Olson and L. Giglio, 1996: A Simplified Scheme for Obtaining Precipitation and Vertical Hydrometeor Profiles from Passive Microwave Sensors. *IEEE Trans. on Geosci. and Rem. Sen.*, **34**, 1213-1232.

Kummerow, C. D., S. Ringerud, J. Crook, D. Randel and W. Berg, 2010. An observationally generated *A-Priori* database for microwave rainfall retrievals, *J. Atmos. and Oceanic Tech.*, **28(2)**, 113-130, doi: 10.1175/2010JTECHA1468.1.

Lorenc, A. C., 1986: Analysis methods for numerical weather prediction. *Quart. J. Royal Met. Soc.*, **112**, 1177-1194.

McCollum, J.R., R. Ferraro, C. Zhou, C. Kummerow, Y. Wang, 1999: The EOS-PM1 AMSR land rainfall algorithm, *J. Geophys. Res.*

Reynolds, R.W., T.M. Smith, C. Liu, D.B. Chelton, K.S. Casey, and M.G. Schlax, 2006: Daily high-resolution-blended analyses for sea surface temperature. *J. Climate,* **20,** 5473- 5496.